HYDROLOGICAL PROCESSES
Hydrol. Process. **29**, 3848–3861 (2015)
Published online 11 May 2015 in Wiley Online Library
(wileyonlinelibrary.com) DOI: 10.1002/hyp.10502

Runoff to boreal lakes linked to land cover, watershed morphology and permafrost thaw: a 9-year isotope mass balance assessment

J. J. Gibson,[1,2]* S. J. Birks,[2,3] Y. Yi[1,2] and D. H. Vitt[4]

[1] *Alberta Innovates Technology Futures, 3-4476 Markham Street, Victoria, BC, V8Z 7X8, Canada*
[2] *University of Victoria, Department of Geography, Victoria, BC, V8W 3R4, Canada*
[3] *Alberta Innovates Technology Futures, 3608-33 St NW, Calgary, Alberta, T2L 2A6, Canada*
[4] *Department of Plant Biology, Southern Illinois University, Carbondale, IL, USA*

Abstract:

Stable isotopes of oxygen and hydrogen were measured in water samples collected annually from a representative suite of 50 lakes in northeastern Alberta over a 9-year period and are interpreted using a steady-state isotope mass balance model to determine water yield and runoff ratios for the lake watersheds and residence time of the lakes. This isotopic perspective on hydrology of the region provides new insight into the role of land cover, watershed morphometry, climatic drivers and permafrost thaw on lakes. Bog cover, permafrost and presence of thaw features in bogs are found to be the dominant hydrologic drivers, although morphometric properties such as elevation, lake area and drainage basin area are also influential. In addition to quantifying the hydrologic fluxes, the analysis establishes contrasting conditions in more southerly lakes, located in the Stony Mountains and west of Fort McMurray, as compared with more northerly sites in the Birch Mountains, Caribou Mountains and northeast of Fort McMurray, mainly because of contributions from thawing permafrost at the northerly sites. Distinct hydrologic conditions are also noted for Shield systems north of Lake Athabasca where bogs and permafrost are absent. While permafrost thaw is not directly labelled by oxygen and hydrogen isotope composition, isotope mass balance calculations suggest that contributions of up to several hundred millimetres per year are occurring in 14 of the 50 lake watersheds under study. Several of these lakes have water yields in excess of precipitation in some years, and regional groups of lakes display significant correlations between water yield and percentage of bogs that have collapsed.

KEY WORDS isotopes; lakes; water balance; evaporation; boreal; bog; fen; permafrost thaw

Received 8 October 2014; Accepted 25 March 2015

INTRODUCTION

Isotope mass balance methods have been progressively applied across northern Canada to study the water balance of lakes and watersheds for both hydrologic characterization and critical loads of acidity assessments (Gibson *et al*., 2005; Birks and Gibson, 2009; see also Yi *et al*., 2008; Brock *et al*., 2009; Wolfe *et al*., 2011; Turner *et al*., 2014). The method has been successful in characterizing hydrology because of systematic isotopic enrichment that occurs in lakes, largely in response to the amount of lake evaporation compared with throughflow generated from the landscape or connected streams. Recent application of the method has focused in part on developing a better understanding of hydrology in the boreal plains region of Alberta in close proximity to oil sands development (Bennett *et al*., 2008; Jeffries *et al*., 2010; Schmidt *et al*., 2010; Scott *et al*., 2010; Gibson *et al*., 2010a,2010b). Short-term water yields have been compared with interpolated runoff from the Water Survey of Canada hydrometric gauging network for this area (Bennett *et al*., 2008), critical loads of acidity have been evaluated based on longer-term interannual datasets (Gibson *et al*., 2010a,2010b) and radon-222 has also been applied to examine the fraction of water yield that is derived from subsurface flowpaths for selected lakes (Schmidt *et al*., 2010). While hydrological conditions in the region have been described, relatively few conclusions have previously been made about the mechanisms that control runoff and water yield. Recent mapping of the land cover characteristics of 50 lake watersheds, with special emphasis on wetland classification by the system outlined in Halsey *et al*. (2003), has shed considerable new light

*Correspondence to: John J. Gibson, Alberta Innovates Technology Futures, 3-4476 Markham Street, Victoria BC V8Z 7X8, Canada.
E-mail: jjgibson@uvic.ca

on the distribution of the land cover units that drive runoff across the region, including bogs, fens, uplands and permafrost terrain that evidently influence the generation of runoff. This lake network, maintained for over 15 years as part of the Regional Aquatics Monitoring Program (RAMP) operated by Alberta Environment and Sustainable Resource Development and the Cumulative Environmental Management Association, has supported collection of lake geochemistry annually since the late 1990s and sampling for stable isotopes since 2002. Here, we describe conditions in the RAMP lakes based on isotopic records collected over a 9-year period, from 2002 to 2010, and provide new insight into the role of land cover, watershed morphometry and permafrost thaw in generating regional runoff. While thawing of permafrost across the region has been described in general (Vitt *et al.*, 1994, 1999), few studies (see Prepas *et al.*, 2001) have examined the relationship between land cover characteristics, morphometry and runoff to lakes in wetland-dominated systems, and none has investigated potential relationships between permafrost conditions and runoff.

Knowledge gained from these investigations is of paramount importance for basic assessment and management of water resources in the region and in particular to better understand and describe the potential effects of climate change and oil sands development in the region.

STUDY SITES

The study lakes are situated in boreal plains and boreal shield regions of northeastern Alberta (Figure 1). Forty of the study lakes are situated within 200 km of Fort

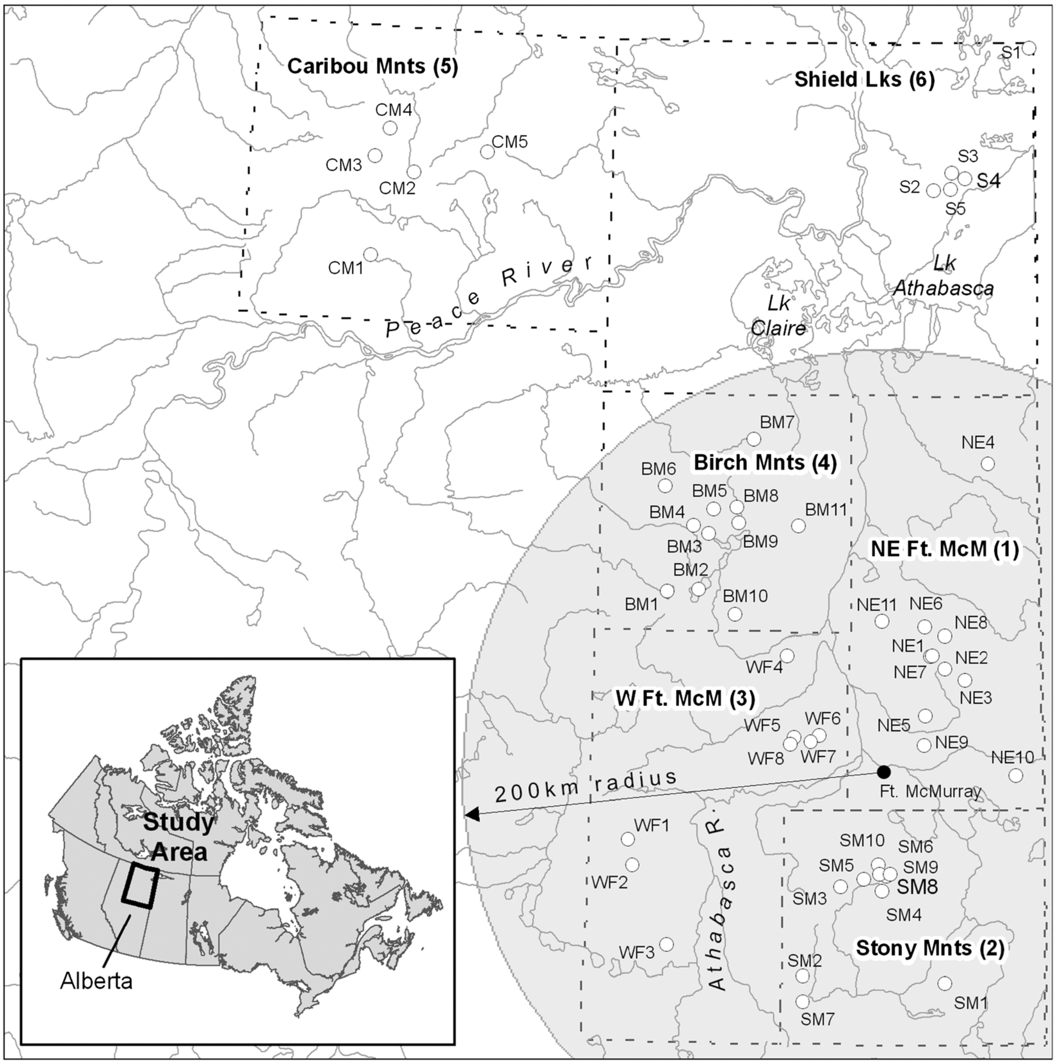

Figure 1. Map showing the location of study lakes relative to the city of Fort McMurray (after Bennett *et al.*, 2008)

McMurray and in close proximity to current oil sands developments. Of these, 11 lakes are located in the Birch Mountains (BM), 11 are situated northeast of Fort McMurray (NE), 8 are situated west of Fort McMurray (WF) and 10 are located in the Stony Mountains (SM). The remaining ten lakes are situated in the Caribou Mountains (CM) and north of Lake Athabasca (S). The lakes are situated in headwater catchments and range in size from small, shallow ponds (1-m depth, $<0.5\,km^2$) to large lakes (30-m depth, $0.43\,km^2$; Bennett *et al.*, 2008). They also vary by latitude, morphometry and associated landscape (Gibson *et al.*, 2010a). Lakes north of Lake Athabasca are underlain at shallow depth by Canadian Shield with a thin mantle of Quaternary deposits. In all other regions, lakes are underlain by Quaternary tills, sandstone, siltstone, shale and carbonates of Cretaceous to Devonian age. Lakes situated in the Stony, Birch and Caribou mountains are distinct in that they are situated on plateaus where the Cretaceous Colorado Shale has weathered recessively and forms a shallow, relatively impervious barrier to vertical groundwater movement.

Land cover is dominated by bog, fen, open water and upland (Table I). Permanent streams rarely occur upstream of lakes but rather tend to form as drainage channels from lake outlets. Several significant statistical correlations were observed for the 50 lakes using Spearman Rank Order tests:

1. %bog is positively correlated with elevation ($r = 0.580$; $p < 0.001$);
2. %upland is negatively correlated with elevation ($r = -0.650$ $p < 0.001$);
3. %bog is negatively correlated with %fen ($r = -0.422$; $p = 0.002$) and %upland ($r = -0.482$; $p < 0.001$); and
4. %fen is negatively correlated with %upland ($r = -0.372$; $p = 0.008$) and %Bog (B) Forest (F) permafrost (X) collapse scar (C) (BFXC) ($r = -0.546$; $p < 0.001$)

In general, these features reflect the fact that bogs occupy higher elevational ranges including the shale-dominated plateaus (SM, BM and CM). Uplands and fens typically occupy lower elevation ranges, fens typically receiving much of their input from bogs. A general rule is that lower elevation areas are either flat with relatively wet fens or sloping with relatively dry uplands. Wetlands occupy between 52% and 97% of watersheds, bogs accounting for up to 75% of terrain in some regions, fens accounting for up to 70% and uplands accounting for up to 44%. Note that %open water (Table I) refers to surface waters other than the lake of interest, and these constitute only a minor fraction of the overall land cover (less than 3%).

Permafrost occurs either as continuous lenses within peatland landforms (termed peat plateaus) or as discontinuous lenses of ice (frost mounds). As permafrost thaws, small rounded to elliptical collapse scars form in association with peat plateaus (BFXC and BTXC-bog treed permafrost collapse scar) or as irregular internal lawns in bog landforms with discontinuous permafrost (BFNI-bog forest no permafrost internal lawn and BTNI –bog treed no permafrost internal lawn; Beilman *et al.*, 2000). Large tracts of permafrost in the area are currently unstable and in disequilibrium with present climate (Vitt *et al.*, 1999). As described by Vitt *et al.* (1994), many bogs in northeastern Alberta contain small, isolated internal wet depressions, collapse scars or internal lawns, which are interpreted as being areas where permafrost has thawed because of climate warming (sometimes in combination with wildfire) resulting in ground subsidence. Commonly dead trees, drunken forests or slumping peat banks are evident from air photos. Other evidence such as layers of woody debris in the peat profile or plant macrofossils indicating drier past conditions has also been observed in these thaw features (Vitt *et al.*, 1994). All bogs are either wooded (open canopy –(T)) or forested (closed canopy –(F)) with *Picea mariana* and abundant ericaceous shrub cover (Vitt *et al.*, 1994). Thaw features, present as wet carpets or lawns with abundant sedges and *Sphagnum*, often form depressions that are up to 1 m below the surrounding permafrost surface. In many cases these depressions are connected to one another and/or to the surrounding wetland landscape through drainage channels.

Table I. Land cover distribution, averages (and ranges) by lake subregion

	n	%Bog	%Fen	%Upland	%Open Water	%Lake
NE	11	8 (0–45)	70 (54–86)	14 (0–47)	0 (0–3)	5 (1–11)
SM	10	4 (0–13)	62 (24–79)	16 (0–54)	3 (0–7)	12 (5–23)
WF	8	2 (0–4)	57 (31–90)	33 (1–61)	3 (0–11)	4 (1–8)
BM	11	38 (0–80)	32 (4–87)	18 (0–39)	0 (0–1)	12 (3–28)
CM	5	75 (65–87)	7 (2–12)	5 (0–21)	1 (1–2)	12 (8–19)
S	5	0 (0–0)	44 (30–57)	44 (31–56)	1 (0–4)	11 (6–22)

n = no. of lakes; %Open Water excludes area of lake (%Lake) considered in IMB.

METHOD

Water sampling

Water samples were collected from float plane or helicopter in 30-ml to 1-l high-density polyethylene bottles with minimal headspace and tightly sealed polypropylene lids to minimize evaporation prior to analysis, which typically occurred within 2 months of collection. In storage trials, such bottles have been shown to be very effective at preventing isotopic fractionation for periods in excess of 1 year (Spangenberg, 2012). Procedures used for water sampling have been described previously (Gibson *et al.*, 2010a,2010b). In general grab samples of water were collected from near the lake centre at approximately 1-m depth during late August to early October. Note that use of grab samples to represent the whole water body presumes that the lakes were well mixed and unstratified. This has been shown to be a reasonable approximation for similar shallow lakes in northern Alberta at this time of year (Gibson *et al.*, 2002).

Groundwater was collected using Solinst™ drive-point piezometers installed with a Pionjar™ percussion hammer using a custom-designed method (see Tattrie, 2011). Surficial permafrost was sampled directly near the shore of BM2 (Namur Lake) from shallow soil cores, whereas permafrost meltwater was obtained from abundant depression-stored water that had ponded at the base of permafrost-cored slopes at BM2 and was evidently also draining to the lake.

All isotope results are reported in δ notation in permil (‰) relative to the Vienna Standard Mean Ocean Water (V-SMOW) and normalized to the SMOW-SLAP scale (see Coplen, 1996). We estimate analytical uncertainty to be better than ±0.1‰ for $\delta^{18}O$ and ±1‰ for $\delta^{2}H$ over the course of the study.

Isotope mass balance

For well-mixed lakes in hydrologic and isotopic steady state, Gibson and Reid (2014) showed that the fraction of water loss by evaporation (x) can be estimated as follows:

$$x = E/I = (\delta_I - \delta_L)/(\delta_E - \delta_L) \text{ (dimensionless)} \quad (1)$$

where I and E are lake inflow and evaporation (m^3/year) and δ_I, δ_L and δ_E are the isotopic compositions of inflow, lake water and evaporation fluxes (‰), respectively. The isotopic composition of evaporate δ_E can be estimated using the Craig and Gordon (1965) model given by Gonfiantini (1986) as follows:

$$\delta_E = ((\delta_L - \varepsilon^+)/\alpha^+ - h\delta_A - \varepsilon_K)/\left(1 - h + 10^{-3}\cdot\varepsilon_K\right) \text{ (‰)} \quad (2)$$

where h is the relative humidity (decimal fraction), δ_A is the isotopic composition of atmospheric moisture, $\varepsilon^+ = (\alpha^+ - 1)\cdot 1000$ is the equilibrium isotopic separation, α^+ is the equilibrium isotopic fractionation (Horita *et al.*, 2008), $\varepsilon_K = C_K(1-h)$ is the kinetic isotopic separation, where C_K is the ratio of molecular diffusivities of the heavy and light molecules and h is humidity. Here, we use C_K values that are representative of fully turbulent wind conditions and a rough surface, i.e. 14.2 for oxygen and 12.5 for hydrogen, based on experimental data (see Horita *et al.*, 2008). Substitution of Equation (2) into Equation (1) yields

$$x = E/I = (\delta_L - \delta_I)/(m(\delta^* - \delta_L)) \text{ (dimensionless)} \quad (3)$$

where

$$m = \left(h - 10^{-3}\cdot(\varepsilon_K + \varepsilon^+/\alpha^+)\right)/\left(1 - h + 10^{-3}\cdot\varepsilon_K\right) \text{ (dimensionless)} \quad (4)$$

and

$$\delta^* = (h\delta_A + \varepsilon_K + \varepsilon^+/\alpha^+)/\left(h - 10^{-3}\cdot(\varepsilon_K + \varepsilon^+/\alpha^+)\right) \text{ (‰)} \quad (5)$$

A partial equilibrium model (Bennett *et al.*, 2008; Gibson and Reid, 2014) is used to estimate the isotopic composition of atmospheric moisture δ_A from isotope composition of precipitation δ_P based on a best fit to the local evaporation line:

$$\delta_A = (\delta_P - k\varepsilon^+)/\left(1 + 10^{-3}\cdot k\varepsilon^+\right) \text{ (‰)} \quad (6)$$

where k typically ranges from 0.5 to 1.

The runoff volume R can also be estimated according to Gibson and Reid (2014) as follows:

$$R = E/x - P - J \quad \left(\text{m}^3/\text{year}\right) \quad (7)$$

where $E = e\cdot LA$ and $P = p\cdot LA$, where e and p representing the annual depth equivalent of evaporation and precipitation (m/year), LA is the lake area (m^2) and J is the inflow from upstream lakes. For headwater lakes where $J = 0$, as is the case for the current network, it follows that

$$R = E/x - P \quad \left(\text{m}^3/\text{year}\right) \quad (7a)$$

which can then be converted to water yield (expressed as depth of runoff from the watershed) as follows

$$WY = R/WA\cdot 1000 \text{ (mm/year)} \quad (8)$$

where WA is the watershed area. Runoff ratio can also be computed as follows:

$$Z = R/P \quad (9)$$

And given that the volume of the reservoir can be estimated, then the residence time of water can estimated as follows:

$$\tau = V/I \text{ or } \tau = xV/E \text{ (year)} \quad (10)$$

Watershed and climate parameters

Wetland site types (bog, fen, peat plateaus (BFXC)), as well as open water and upland polygons, were delimited using 1 : 20 000 black and white photography. Definitions of site types follow those of Halsey *et al.* (2003). Using ArcGIS, areas of the various site types, watershed areas (*WA*) and lake areas (*LA*) for each of the study lakes were estimated (Table II), and drainage basin areas were calculated ($DBA = WA - LA$). Climatological parameters required to run the isotope mass balance (i.e. precipitation, temperature, relative humidity, evaporation and precipitation rates) were obtained by interpolation from the North American Regional Reanalysis (NARR) dataset (Mesinger *et al.*, 2006) as discussed previously in Gibson *et al.* (2010a,b).

RESULTS AND DISCUSSION

Isotope characteristics

Isotope data for lakes are summarized in Table III and Figure 2. As shown, isotope data plot below the Global Meteoric Water Line (GMWL) in δ^2H–δ^{18}O space (Figure 2), which has been widely observed for evaporating water bodies sampled in the region (Bennett *et al.*, 2008; Gibson *et al.*, 2010a,2010b), as well as across much of continental northern Canada (Gibson *et al.*, 2005). Evaporation line (LEL) slopes determined by linear regression are found to be fairly consistent, ranging from about 5.3 to 5.5 from year to year. Offset below the GMWL along evaporation lines is proportionate to the fraction of water loss by evaporation from each lake, with seasonality in inflow and evaporation rates contributing to variability in the degree of offset.

The mean isotopic composition of precipitation δ_P is estimated for each lake location based on empirically derived relationships between latitude, elevation and isotope composition across North America (Bowen and Wilkinson, 2002). As described previously (Gibson *et al.*, 2010a,2010b), these interpolations were performed using long-term average climatologies, and the δ^2H of monthly precipitation was calculated assuming that precipitation would follow the relationship defined by the GMWL (Craig, 1961). Overall, the isotope composition of precipitation is predicted to vary latitudinally, ranging from −17.80‰ for $\boldsymbol{\delta}^{18}$O and −132.1‰ for $\boldsymbol{\delta}^2$H for southernmost lakes (SM) to −19.80‰ for $\boldsymbol{\delta}^{18}$O and −148.4‰ for $\boldsymbol{\delta}^2$H for northernmost lakes (CM; Table IV). Limited sampling of precipitation was also carried out at selected sites (see Bennett, 2006; Tattrie, 2011) although precipitation samples were evidently affected by evaporation from the sampler and so are not used.

Groundwater, permafrost and permafrost meltwater are found to be very similar to the modelled isotopic composition of precipitation. As shown in Figure 2, groundwater (1- to 10-m depth) and surficial permafrost (~1-m depth) plot very slightly below the GMWL but typically lie between the LWML for Edmonton and the GMWL. Evaporation from soils or evaporation from standing water prior to recharge may have an influence on the resulting isotopic signatures. As shown for sites in SM, BM and NE, groundwaters and permafrost are generally within 0.5‰ for $\boldsymbol{\delta}^{18}$O and 5‰ for $\boldsymbol{\delta}^2$H of modelled mean annual precipitation (Table V), which is an important constraint to consider when reviewing the isotope mass balance model outputs in the following sections.

Model setup and outputs

Using isotopic compositions of the lakes on a year-by-year basis and long-term averages modelled for isotopic composition of precipitation at each site and using basic climatological data, we estimate evaporation/inflow (x) from Equation (3), water yield from Equation (8), runoff ratio from Equation (9) and water residence time from Equation (10). A single best fit for all lakes and years is used to solve for k (0.40) in Equation (6). Note that the use of mean annual δ_P to represent bulk water inflow to the lakes by a combination of direct precipitation, surface runoff, groundwater and permafrost meltwater is a necessary model simplification, but because of isotopic similarity of these sources, this assumption only introduces a 3% to 4% uncertainty in calculated hydrologic quantities. As the isotopic composition of groundwater and permafrost meltwater falls slightly below the GMWL (Figure 2, inset), this assumption is likely to overestimate E/I and residence time and underestimate water yield and runoff ratio. It is important to note that water yield derived using this approach is a combined measure of surface water and groundwater input to the lakes but does not differentiate between the two fluxes.

An overall impression of the variability of the results for the 50 lakes over the 9-year period is provided in Figure 3. Estimates of water yield values for individual lakes by year are given in Table II. As expected compared with previous assessments (see Gibson *et al.*, 2010a,2010b), evaporation/inflow and water yield (and runoff ratio, not shown) produce distributions that are positively skewed (Figure 3). In other words the majority of lake systems tend to have less dynamic hydrology (i.e.

Table II. Lake area, watershed area, estimated water yields (mm/year) with basic statistics

	Lake area (km^2)	Watershed area (km^2)	2002	2003	2004	2005	2006	2007	2008	2009	2010	Mean	Stdev
NE1	0.65	16.10	197	194	133	265	180	98	383	201	88	193	90
NE2	0.34	14.79	153	111	79	152	161	66	146	130	94	121	35
NE3[a]	1.16	22.82	88	132	112	232	248	58	140	136	104	139	63
NE4	0.58	2.59	606	503	449	869	409	260	587	708	369	529	186
NE5[a]	1.89	5.43	267	488	379	480	303	101	410	560	426	379	139
NE6	0.37	7.97	156	148	91	260	101	192	42	155	282	159	78
NE7	0.11	5.80	166	125	101	162	126	132	172	121	140	138	24
NE8[a]	0.11	0.71	753	586	373	861	461	349	985	669	831	652	226
NE9[a]	3.15	8.06	176	245	255	339	319	106	279	491	354	285	110
NE10	4.19	12.90	132	128	230	373	246	189	245	426	240	245	99
NE11	5.75	71.42		167	140	239	112	47	129	144	96	134	56
SM1	2.37	7.24	132	181	230	277	143	49	387	383	314	233	117
SM2	1.97	13.38	31	33	72	126	65	10	129	141	118	80	50
SM3	1.86	5.53	182	260	236	433	296	211	359	428	374	309	93
SM4	0.53	11.22	29	73	57	72	69	58	88	97	86	70	20
SM5	1.06	2.61	241	258	260	347	274	218	587	525	506	357	142
SM6	0.70	12.36	39	51	60	84	69	53	86	84	74	67	17
SM7	1.48	5.46	56	117	142	193	171	116	295	338	263	188	93
SM8	1.91	7.72	144	213	230	323	256	70	326	314	278	239	87
SM9	1.07	7.21	156	205	204	412	259	225	289	266	256	253	72
SM10	1.35	16.83	95	124	136	135	149	90	195	197	154	142	38
WF1	3.20	7.23	98	235	252	305	218	200	523	427	311	285	127
WF2	0.76	3.55	46	96	81	182	69	−25	232	161	119	107	77
WF3	2.16	49.39	19	35	51	91	43	34	101	88	44	56	29
WF4	0.03	1.76	9	8	10	78	17	9	29	28	16	23	22
WF5	0.23	4.81	14	38	30	156	49	34	62	68	81	59	42
WF6	0.18	4.01	27	99	77	196	81	61	78	133	121	97	49
WF7	0.09	1.51	34	138	73	214	105	62	115	174	173	121	59
WF8	2.03	21.06	20	42	38	93	61	25		95	39	52	29
BM1[a]	17.03	41.69	431	660	595	435	607	343	703	697	615	565	130
BM2[a]	43.97	121.57	353	536	472	410	487	263	551	577	518	463	103
BM3	0.97	28.79	77	141	87	168	112	59	134	182	97	117	42
BM4	4.26	33.07	167	232	119	455	274	112	303	422	270	262	121
BM5	2.64	27.95	141	244	118	455	232	92	262	322	162	225	114
BM6[a]	1.29	12.38	393	455	285	733	407	284	429	570	521	453	141
BM7[a]	0.68	3.98	430	444	531	514	287	245	351	509	365	408	103
BM8	1.22	31.28	121	168	101	289	151	69	115	213	114	149	67
BM9	3.48	29.78	179	288	246	295	326	239	278	311	248	268	45
BM10	0.39	4.76	30	25	27	92	51	33	76	192	50	64	53
BM11	0.06	0.52	75	117	121	133	116	69	79	130	87	103	25
CM1[a]	1.60	22.51	240	310	235	378	455	551	728	603	545	449	171
CM2[a]	9.55	37.22	304	328	234	447	404	328	401	485	452	376	82
CM3[a]	2.30	25.65	189	162	111	331	275	249	220	346	285	241	78
CM4[a]	2.63	35.42	242	275	182	219	228	308	394	503	383	304	104
CM5[a]	0.55	2.23	225	212	136	697	704	175	212	391	408	351	218
S1	3.40	9.99	425	482	387	389	452	349	502	438	424	428	48
S2	1.03	111.56	43	51	42	65	39	—	54	71	33	50	13
S3	1.45	36.44	112	159	130	140	148	139	150	187	115	142	23
S4	1.42	113.23	23	30	24	57	38	38	42	39	28	36	11
S5	0.32	4.16	113	122	108	116	127	—	118	144	81	116	18

[a] Lakes apparently fed by permafrost thaw.

lower runoff) while few systems display a more dynamic response. Water residence times for the lakes were found to range from less than 2 months to greater than 9 years, with average residence times greater than 1 year in most subregions (Table VI). The fact that these lakes are not completely hydrologically flushed on an annual scale promotes isotopic stability both seasonally and from year to year and importantly justifies the use of a steady-state isotope balance model in the current application. We use Spearman Rank Order as a correlation method in this

Table III. Oxygen-18 and deuterium isotopic composition of lakes sampled during 2002–2010 (‰V-SMOW)

	2002		2003		2004		2005		2006		2007		2008		2009		2010	
	$\delta^{18}O$	$\delta^{2}H$	$\delta^{18}O$	$\delta^{2}H$	$\delta^{18}O$	$\delta^{2}H$	$\delta^{18}O$	$\delta^{2}H$	$\delta^{18}O$	$\delta^{2}H$	$\delta^{18}O$	$\delta^{2}H$	$\delta^{18}O$	$\delta^{2}H$	$\delta^{18}O$	$\delta^{2}H$	$\delta^{18}O$	$\delta^{2}H$
NE1	−16.1	−130.4	−15.2	−125.7	−14.5	−126.2	−15.8	−133.0	−14.8	−126.3	−13.3	−119.5	−16.5	−129.6	−14.5	−126.2	−13.2	−116.7
NE2	−16.6	−137.7	−15.2	−123.5	−14.6	−127.7	−15.9	−133.1	−15.9	−133.1	−13.8	−121.8	−15.8	−127.4	−14.6	−127.7	−14.9	−124.2
NE3	−12.9	−117.1	−13.1	−113.4	−13.0	−118.3	−14.6	−126.5	−14.6	−126.5	−10.7	−107.6	−13.3	−114.6	−13.0	−118.3	−12.4	−112.3
NE4	−15.0	−128.1	−14.2	−125.9	−14.2	−128.4	−15.6	−132.0	−13.5	−123.2	−12.3	−115.1	−14.5	−123.2	−14.2	−128.4	−13.2	−120.0
NE5	−10.8	−108.5	−11.5	−107.2	−11.1	−108.2	−11.3	−109.5	−10.0	−103.6	−8.0	−94.8	−10.9	−102.7	−11.1	−108.2	−10.9	−106.7
NE6	−15.2	−127.9	−14.2	−123.0	−13.1	−121.2	−15.5	−131.5	−12.9	−119.2	−14.9	−122.7	−10.5	−102.7	−13.1	−121.2	−15.8	−130.0
NE7	−17.0	−136.1	−15.8	−129.4	−15.6	−129.9	−16.3	−135.4	−15.7	−127.4	−15.8	−128.0	−16.4	−130.7	−15.6	−129.9	−16.1	−131.4
NE8	−15.9	−131.9	−14.5	−124.6	−13.6	−121.5	−15.4	−131.0	−13.8	−122.7	−13.1	−118.5	−15.8	−125.8	−13.6	−121.5	−15.5	−127.7
NE9	−9.1	−94.1	−9.1	−93.9	−9.6	−100.7	−9.8	−101.7	−9.7	−99.6	−7.8	−94.2	−9.4	−99.5	−9.6	−100.7	−10.0	−100.6
NE10	−8.7	−93.5	−8.1	−91.8	−9.8	−101.4	−10.5	−105.4	−9.5	−101.5	−9.0	−96.3	−9.4	−97.4	−9.8	−101.4	−9.3	−97.0
NE11	—	—	−12.6	−116.0	−12.3	−114.9	−13.5	−120.7	−11.2	−111.0	−9.0	−101.5	−11.7	−109.3	−12.3	−114.9	−10.9	−106.3
SM1	−8.4	−91.2	−8.3	−89.9	−9.3	−96.6	−9.4	−99.3	−8.3	−91.5	−7.2	−88.8	−10.1	−97.3	−9.3	−96.6	−9.6	−97.9
SM2	−7.2	−87.3	−7.0	−81.6	−8.9	−95.1	−9.7	−101.1	−8.5	−92.5	−7.2	−88.6	−9.6	−94.0	−8.9	−95.1	−9.4	−97.7
SM3	−9.6	−99.3	−9.7	−99.0	−9.9	−100.6	−11.0	−107.9	−10.1	−100.6	−9.5	−99.1	−10.5	−102.5	−9.9	−100.6	−10.6	−106.4
SM4	−10.0	−101.3	−11.7	−106.2	−11.3	−106.3	−11.5	−110.7	−11.4	−106.8	−11.0	−106.1	−12.1	−109.6	−11.3	−106.3	−12.1	−111.3
SM5	−9.9	−100.0	−9.3	−97.6	−9.7	−99.7	−9.9	−102.3	−9.5	−99.7	−9.2	−98.0	−11.3	−104.6	−9.7	−99.7	−11.0	−105.9
SM6	−10.3	−101.8	−10.2	−102.8	−10.9	−105.4	−11.4	−110.1	−10.9	−104.4	−10.4	−103.0	−11.5	−104.3	−10.9	−105.4	−11.1	−106.7
SM7	−7.2	−89.3	−7.9	−89.9	−9.0	−97.8	−9.1	−98.2	−9.1	−95.5	−8.6	−95.1	−10.1	−98.7	−9.0	−97.8	−9.9	−100.9
SM8	−9.8	−100.0	−10.0	−101.4	−10.6	−105.2	−11.1	−108.2	−10.5	−101.3	−8.3	−95.6	−11.1	−101.7	−10.6	−105.2	−10.6	−104.4
SM9	−11.7	−109.4	−11.4	−105.1	−11.6	−108.5	−13.3	−119.9	−11.9	−107.8	−11.6	−109.1	−12.2	−110.7	−11.6	−108.5	−12.0	−112.2
SM10	−12.1	−112.4	−11.7	−108.3	−12.3	−113.8	−11.8	−112.2	−12.1	−108.6	−10.8	−105.0	−12.9	−110.9	−12.3	−113.8	−12.3	−113.6
WF1	−7.4	−89.9	−8.8	−97.2	−9.3	−100.5	−9.3	−99.1	−8.8	−96.5	−8.5	−95.8	−11.1	−101.3	−9.3	−100.5	−9.3	−99.8
WF2	−7.4	−87.9	−8.4	−94.3	−8.5	−96.7	−9.8	−101.8	−8.1	−95.5	−6.5	−87.7	−10.4	−100.6	−8.5	−96.7	−8.7	−95.6
WF3	−8.4	−92.7	−9.3	−98.2	−10.8	−105.5	−12.1	−113.6	−10.0	−101.2	−9.7	−102.7	−12.3	−110.4	−10.8	−105.5	−10.0	−101.2
WF4	−9.0	−105.2	−8.0	−96.9	−8.9	−105.1	−14.1	−124.1	−9.8	−104.3	−8.6	−99.4	−11.3	−111.7	−8.9	−105.1	−9.7	−105.9
WF5	−8.4	−99.1	−9.7	−103.8	−9.5	−103.2	−13.6	−121.5	−10.3	−105.2	−9.7	−102.4	−11.0	−106.9	−9.5	−103.2	−11.8	−111.8
WF6	−10.0	−104.8	−12.6	−113.5	−12.1	−116.7	−14.4	−125.6	−11.8	−111.8	−11.1	−110.3	−11.7	−115.0	−12.1	−116.7	−13.2	−118.9
WF7	−10.2	−106.7	−13.0	−110.0	−11.4	−114.9	−14.1	−124.0	−12.0	−113.7	−10.6	−108.8	−12.3	−116.3	−11.4	−114.9	−13.7	−121.5
WF8	−7.9	−93.9	−8.4	−91.6	−8.7	−94.7	−10.1	−103.2	−9.3	−100.3	−8.1	−95.3	—	—	−8.7	−94.7	−9.4	−99.3
BM1	−12.5	−114.2	−12.9	−116.6	−12.7	−115.7	−11.3	−109.4	−12.4	−112.4	−10.8	−108.7	−12.8	−114.4	−12.7	−115.7	−12.6	−114.6
BM2	−12.2	−114.6	−12.5	−112.8	−12.3	−113.0	−11.4	−109.8	−12.0	−111.3	−10.4	−106.9	−12.3	−112.6	−12.3	−113.0	−12.3	−112.4
BM3	−14.3	−124.9	−15.5	−133.1	−14.4	−130.0	−15.7	−132.4	−14.7	−123.6	−12.9	−118.2	−15.2	−130.1	−14.4	−130.0	−14.6	−126.9
BM4	−12.5	−112.1	−13.1	−122.2	−11.3	−112.8	−14.8	−127.6	−13.4	−115.3	−10.9	−108.8	−13.7	−122.5	−11.3	−112.8	−13.6	−120.5
BM5	−13.0	−117.9	−14.2	−125.7	−12.3	−117.2	−15.7	−132.1	−13.9	−119.8	−11.2	−110.5	−14.2	−125.0	−12.3	−117.2	−13.2	−117.7
BM6	−15.7	−131.0	−15.7	−135.9	−14.5	−129.4	−16.5	−136.4	−15.1	−124.4	−14.2	−124.2	−15.2	−130.5	−14.5	−129.4	−16.0	−131.5
BM7	−14.7	−125.6	−14.4	−125.4	−15.1	−130.5	−14.7	−127.2	−13.0	−118.5	−12.6	−116.8	−13.6	−120.7	−15.1	−130.5	−14.2	−122.2
BM8	−15.2	−128.4	−15.5	−133.4	−14.4	−128.6	−16.5	−136.7	−15.2	−125.4	−13.0	−118.7	−14.5	−131.7	−14.4	−128.6	−14.8	−124.8
BM9	−13.2	−116.7	−14.2	−124.8	−14.0	−123.1	−14.1	−123.8	−14.4	−122.9	−13.6	−121.4	−14.0	−123.6	−14.0	−123.1	−14.0	−122.7
BM10	−9.0	−101.9	−8.1	−96.3	−8.6	−98.5	−11.0	−107.8	−9.6	−103.5	−8.8	−96.6	−10.6	−103.6	−8.6	−98.5	−9.5	−101.7
BM11	−10.9	−110.1	−11.7	−114.2	−12.1	−114.8	−11.9	−112.3	−11.6	−112.0	−10.4	−106.3	−10.6	−111.1	−12.1	−114.8	−11.2	−110.4
CM1	−16.0	−134.3	−16.4	−134.2	−16.1	−136.7	−16.8	−137.9	−17.1	−138.6	−17.5	−142.2	−17.8	−142.8	−16.1	−136.7	−17.3	−141.0
CM2	−13.5	−120.9	−13.3	−120.2	−12.9	−118.2	−14.3	−125.0	−14.0	−124.1	−13.6	−123.6	−13.9	−123.5	−12.9	−118.2	−14.2	−125.9

CM3	−15.2	−130.9	−14.3	−128.4	−13.7	−125.3	−16.4	−135.9	−15.8	−134.4	−15.7	−133.7	−15.2	−131.1	−13.7	−125.3	−15.8	−137.0
CM4	−16.3	−138.1	−16.4	−136.3	−15.8	−135.9	−15.8	−135.9	−15.8	−135.9	−16.7	−138.4	−17.1	−141.4	−15.8	−135.9	−17.0	−140.7
CM5	−12.7	−116.9	−12.0	−115.1	−11.3	−112.4	−15.6	−131.9	−15.6	−131.9	−11.9	−115.6	−12.1	−115.1	−11.3	−112.4	−13.9	−124.4
S1	−12.3	−115.0	−12.5	−116.2	−12.1	−116.5	−12.1	−113.4	−12.2	−116.1	−11.6	−115.1	−12.7	−115.6	−12.1	−116.5	−12.2	−114.3
S2	−15.6	−132.1	−15.8	−134.8	−15.8	−136.6	−16.4	−136.2	−15.3	−132.6	—	—	−16.0	−137.4	−15.8	−136.6	−15.2	−130.6
S3	−14.5	−127.4	−15.2	−131.9	−15.1	−132.3	−15.1	−132.3	−15.1	−132.3	−15.1	−131.1	−15.2	−133.4	−15.1	−132.3	−14.7	−129.3
S4	−13.1	−120.7	−13.8	−125.6	−13.6	−125.7	−15.6	−132.1	−14.5	−128.9	−14.7	−129.2	−14.9	−131.2	−13.6	−125.7	−13.9	−125.4
S5	−12.5	−116.7	−12.5	−121.8	−12.7	−123.1	−12.7	−123.1	−12.7	−123.1	—	—	−12.5	−118.7	−12.7	−123.1	−11.5	−112.0

paper because of skewness of the hydrological indicators. More details on the water yield and runoff ratios by year and subregion are discussed in the following section.

Water yield and runoff ratio

Water yields are shown for each lake subregion over time compared with annual precipitation interpolated from the NARR dataset (Figure 4). In general water yield is 19% to 75% of estimated precipitation, as shown by calculated runoff ratios (Table VI). For SM, WF and S regions, average runoff ratios range from about 0.19 to 0.37, but tend to be higher for NE, BM and CM, ranging from 0.5 to 0.75. For these higher water yield regions, BM and CM, in particular, water yield is found at times to exceed precipitation. While it is possible that precipitation may be underestimated in our interpolation because of lack of monitoring stations on the shale plateaus, it is also very likely, as discussed later on, that some quantity of additional water is being input to the lakes by thawing of permafrost. While interannual variability in water yield is substantial (Figure 4), no unidirectional temporal trends (either increasing or decreasing) are evident.

Kienzle and Mueller (2013) presented an analysis of water yield based on Water Survey of Canada streamflow data from 1971 to 2000 for 287 larger watersheds across Alberta, including the current study area. Based on their assessment, which is summarized as a map (their Figure 2), it appears that annual water yield ranged between about 60 and 150 mm across our study region. Similar water yields were estimated from previous long-term assessments based on essentially the same monitoring network (Canada, Energy Mines and Resources, 1978). The primary difference between previous studies and our own is that of spatial footprint; while we calculate annual values over a somewhat shorter time period of 9 years, we focus on areas that are typically an order of magnitude smaller than the streamflow gauging network and therefore capture more spatial variability in runoff. As a result, mean annual water yield to individual lakes was found in our assessment to range from 36 to 652 mm. One of the most interesting advantages of smaller spatial footprint (ours ranging from <1 to 122 km^2) is that we can look at the influence of land cover on the hydrology of the system, as we show later on. One additional study we note is that of Quinton and Hayashi (2008), conducted in similar wetland-dominated terrain with discontinuous permafrost in the upper Mackenzie River Valley near Fort Simpson, NT. They estimated annual water yield in four wetland-dominated basins (152 to 2000 km^2) to range from 108 to 168 mm. Although that system has somewhat lower rainfall than our study region, the runoff ratios they report range from 21% to 35%, not very different than our results for the lowland non-shield subregions (SM and

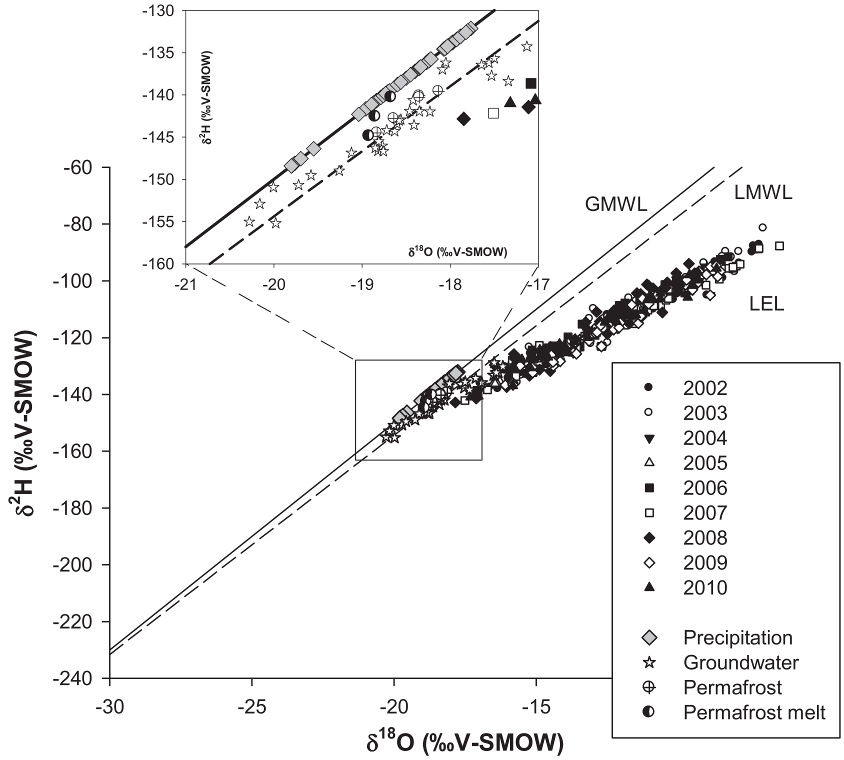

Figure 2. Plot of oxygen-18 *versus* deuterium for lakes, groundwater and permafrost sampled during this study, as well as precipitation interpolated from existing regional datasets. GMWL and local meteoric water line (LMWL) for Edmonton are also shown for reference

Table IV. Mean latitude, longitude and isotopic composition of precipitation by lake subregion

	n	Latitude	Longitude	δ^{18}O (‰V-SMOW)	δ^{2}H (‰V-SMOW)
NE	11	57.1	−110.8	−18.2 (−18.8 to −17.8)	−135.6 (−140.3 to −132.6)
SM	10	56.1	−111.3	−18.1 (−18.3 to −17.8)	−135.1 (−136.1 to −132.1)
WF	8	56.6	−112.3	−18.0 (−18.1 to −17.8)	−134.0 (−134.6 to −132.4)
BM	11	57.7	−112.5	−18.8 (−19.0 to −18.4)	−140.3 (−142.3 to −137.2)
CM	5	59.1	−115.2	−19.7 (−19.8 to −19.5)	−147.8 (−148.4 to −146.4)
S	5	59.3	−110.6	−18.6 (−18.8 to −18.5)	−138.7 (−140.7 to −137.6)

n = no. of lakes; values in brackets indicate range of modelled values for lakes.

Table V. Precipitation, groundwater, permafrost and permafrost-derived meltwater characteristics for selected basins

Water type	Location	*n*	δ^{18}O (‰V-SMOW)	δ^{2}H (‰V-SMOW)
Precipitation	NE7	1	−18.34	−136.7
Groundwater	NE7	23	−18.63 (0.89)	−144.3 (5.7)
Precipitation	SM8	1	−18.24	−136.0
Groundwater	SM8	14	−17.73 (1.26)	−138.2 (7.3)
Precipitation	BM2	1	−18.71	−139.7
Permafrost	BM2	5	−18.46 (0.27)	−141.5 (2.1)
Thawwater	BM2	3	−18.81 (0.13)	−142.6 (2.3)

n = no. of samples; values in brackets are 1 standard deviation; groundwater was collected in piezometers (1- to 10-m depth); permafrost was sampled by shallow coring; meltwater occurred as depression storage at base of permafrost slopes. Precipitation was interpolated based on regional datasets.

WF, see Table VI). While Quinton and Hayashi (2008) do not report any first-hand evidence of collapse scars or systematic thawing, based on review of their aerial photographs (their Figure 2), we believe that the flat bogs they describe feeding the channel fens may be areas similar to our collapse scars where permafrost may be actively degrading.

In the following sections, we further explore the relationship between hydrologic indicators, permafrost, land cover, morphometry and climate using the 9-year average results for the water balance of the lake systems.

Hydrological drivers

A PCA analysis (Figure 5) was conducted to better understand the relationship between the hydrology of the

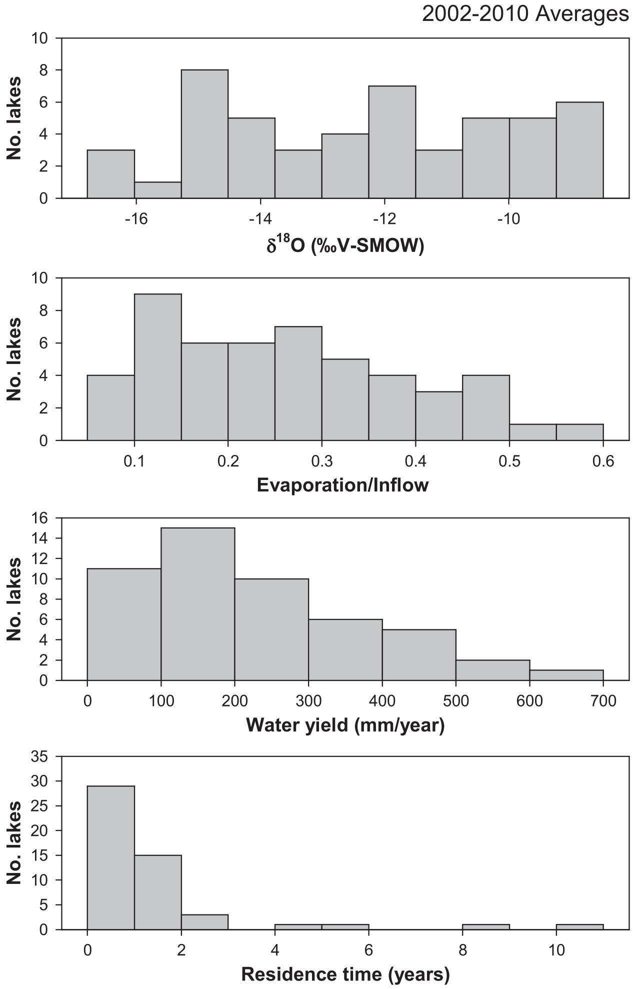

Figure 3. Plots showing the distribution of (i) $\delta^{18}O$; (ii) evaporation/inflow, x; (iii) water yield, WY (a.k.a. runoff); and (iv) water residence time, τ, for the 50 study lakes based on 2002–2010 averages

system and major climatic and land cover drivers in the various subregions. Variations along the PC1 axis accounted for 41% of variability in the dataset, and variations along PC2 accounted for 15% of variability in the dataset. Variations along PC1 correspond mainly to the influence of bog and fen coverage as well as permafrost that in this region occurs exclusively in bogs. Upland cover tends to be more influential for variations along PC2, and open water tends to be the least influential for both axes, as it plots closer to the origin. Variables that seem to influence both axes include the climatic drivers (temperature, precipitation and evaporation), morphometry (LA, elevation and to some extent DBA) and hydrology (water yield, runoff ratio and residence time). Overall, the PCA reveals distinct clustering of subregion groups suggesting similarity among nearby lakes. Very distinct clusters are noted for CM and S lakes, whereby CM lakes are separated mainly by their greater extent of bog cover and permafrost in their catchment areas, and shield lakes, which lack bogs, are driven more by %upland, elevation, LA, and DBA. WF and SM lakes show strong influence of %fen as well as the climatic condition drivers. BM and NE lakes appear somewhat more variable and range between other types. The inset (Figure 5) also shows the distribution of lakes that are suspected to be fed by permafrost thaw, as discussed later on.

Using a Spearman Rank Order test, water yield is found to be correlated with LA ($r = 0.413$, $p < 0.001$) and elevation ($r = 0.431$, $p = 0.002$) and negatively correlated with evaporation ($r = -0.302$, $p = 0.03$) and temperature ($r = -0.353$, $p = 0.01$). In terms of land cover, water yield is strongly correlated with %bog ($r = 0.525$, $p < 0.001$), % permafrost (0.525, $p < 0.001$) and %BFXC (0.525, $p < 0.001$) and negatively correlated with %upland ($r = -0.464$, $p < 0.001$).

Runoff ratios were found to be driven by very similar factors yielding similar but somewhat stronger correlations: LA ($r = 0.429$, $p = 0.002$), elevation (0.428, $p = 0.002$), evaporation ($r = -0.423$, $p = 0.002$), precipitation (−0.359, $p = 0.01$), temperature ($r = -0.469$, $p < 0.001$), %bog (0.525, $p < 0.001$), %permafrost (0.554, $p < 0.001$) and % BFXC (0.571, $p < 0.001$).

Again, bog, permafrost and bog-forest collapse scar terrain are most strongly correlated with the hydrologic fluxes. Water residence times were found to be

Table VI. Average (minimum, maximum) residence time, water yields and estimated runoff ratios by lake subregion (values for permafrost thaw group also shown)

	n	Residence time (year)	Water yield (mm/year)	Runoff ratio (unitless)
NE	11	0.71 (0.14 to 2.04)	270 (121 to 652)	0.50 (0.22 to 1.21)
SM	10	1.40 (0.45 to 2.80)	194 (67 to 357)	0.35 (0.12 to 0.64)
WF	8	1.09 (0.57 to 1.92)	100 (23 to 285)	0.19 (0.04 to 0.59)
BM	11	1.64 (0.13 to 9.03)	280 (64 to 565)	0.57 (0.12 to 1.09)
CM	5	1.68 (0.80 to 2.45)	344 (241 to 449)	0.75 (0.53 to 0.93)
S	5	1.83 (0.64 to 5.35)	154 (36 to 428)	0.37 (0.09 to 1.02)
Non-thaw lakes	36	1.1 (0.14 to 5.35)	161 (23 to 428)	0.31 (0.04 to 1.04)
Thaw lakes	14	2.02 (0.13 to 9.03)	390 (139 to 652)	0.78 (0.25 to 1.20)

n = no. of lakes; values in brackets indicate range of annual modelled values for lakes.

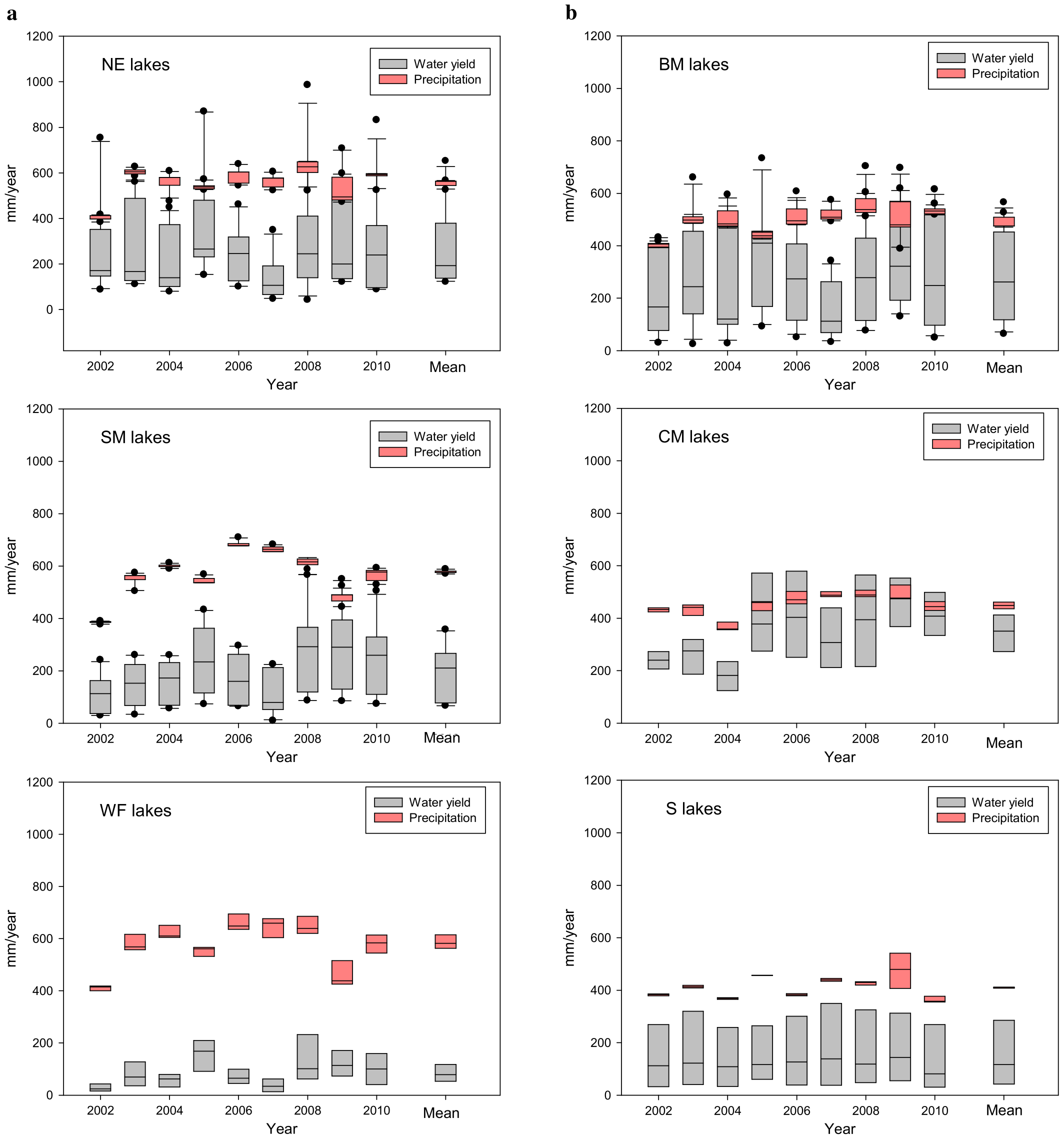

Figure 4. (a, b) Box plots showing water yield values computed for various lake subregions compared with annual precipitation amounts. The boundary of the box closest to zero indicates the 25th percentile, a line within the box marks the median and the boundary of the box farthest from zero indicates the 75th percentile. Whiskers (error bars) above and below the box indicate the 90th and 10th percentiles. Outliers are also shown where number of observations permit

dependent only on LA ($r = 0.550$, $p < 0.001$), consistent with lake size and depth being the major control, and % open water ($r = 0.338$, $p = 0.01$), which could reflect some influence from delayed water movement off the catchment upstream of the lake or may simply indicate watersheds with greater surface roughness that creates ponding.

It is also interesting to note that raw oxygen-18 data from the lakes (and deuterium, not shown) is correlated with residence time ($r = 0.443$, $p = 0.001$) but is not significantly correlated with either water yield or runoff ratio. This attests to the need for employing an isotope mass balance model to gain insight into runoff from watersheds to the lakes.

Influence of thawing permafrost

We have demonstrated that BFXC, permafrost and bog area are the strongest correlates with water yield and runoff ratios, which suggests a systematic link between areas of thawing permafrost and runoff. The strongest evidence for impact of permafrost thawing on water yield is found in areas with greater than 3%bog cover, in high elevation areas of BM, in CM and some lakes within NE. These areas plot in a distinct group in Figure 6, characterized in most cases by high BFXC/bog (i.e. % bog that shows evidence of collapse scars) and higher water yield (Figure 6). In contrast, low elevation areas of BM and all WF and SM sites have relatively low BFXC/bog and significantly lower water yield (Figure 6).

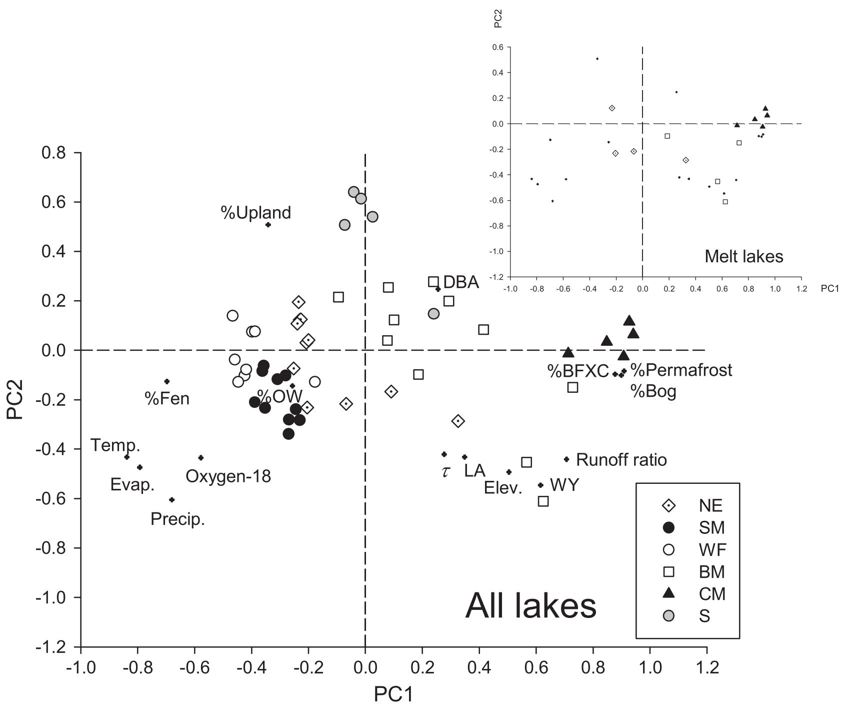

Figure 5. PCA biplot showing lakes differentiated by subregion and overlain by score plot for major variables tested in the analysis. Inset shows subset of lakes apparently influenced by permafrost thawing. Variations along PC1 correspond mainly to differences in %Bog, %Fen, %Permafrost and %BFXC, whereas variations along PC2 incorporate variations in many factors including %Upland, Elevation, DBA and LA. Note that the major climate drivers plot in the lower left quadrant and derived hydrologic variables (water yield, runoff ratio and residence time) plot in the lower right quadrant. Note also that raw oxygen-18 or deuterium (not shown) are not significantly correlated with the derived hydrologic variables (see text for discussion)

Note that BM lakes below 700 m elevation (ranging from 556 to 685 m) fall into the low BFXC/bog and low water yield group, whereas BM lakes greater than 700 m elevation (ranging from 721 to 787 m) fall into the other group. In the high water yield areas, significant negative correlations are found between the BFXC/bog and water yield (Figure 6), suggesting that more runoff occurs from systems where the residual amount of intact (unthawed) permafrost is higher. This would be the case where permafrost is a source of runoff, and contributions wane in locations where permafrost has been more extensively thawed out. It is notable that for many lakes in the high water yield group shown in Figure 6 that estimated water yield may exceed precipitation in some years. For BM1, this is the case in 7 of 9 years, for BM2 in 1 of 9 years, for CM1 in 2 of 9 years and for both NE4 and NE8 in 5 of 9 years. The mean water yield for the 14 lakes apparently affected by permafrost thaw is 390 mm/year (ranging from 139 to 652 mm/year) as compared with water yield in other lakes of 161 mm/year. Mean runoff ratio is 0.80 (0.25 to 1.20) as compared with 0.31 for other lakes, and residence time is 1.9 years (0.13 to 9 years), compared with 1.1 years for other lakes (Table VI). By comparison we find that water yield may be enhanced by up to several hundred millimetres per year and sustained over almost a decade of observation because of thawing of permafrost, with direct evidence of collapse of permafrost in these basins being an important constraint on this interpretation.

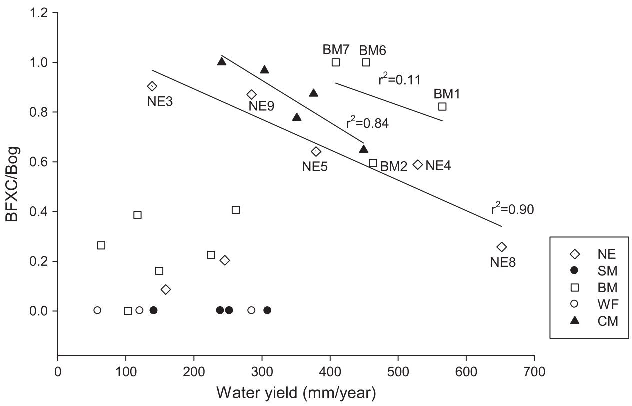

Figure 6. Crossplot showing ratio of bog terrain with collapse scars to total bog area *versus* water yield, for watersheds with bog cover greater than 3%. Note that no lakes from the S (Shield) group meets this criteria. Two distinct responses are observed, including low BFXC/Bog with low water yield and higher BFXC/Bog with higher water yield. Note that BM lakes below 700 m elevation (ranging from 556 to 685 m) fall into the first grouping, whereas BM lakes greater than 700 m elevation (ranging from 721 to 787 m) fall into the latter group. The negative correlation observed in the latter grouping is inferred to be evidence of progressive stages of permafrost thaw in each subregion enhancing water yield, whereby runoff amounts are greater in watersheds with a greater proportion of unthawed areas

Overall, it is evident that the thawing of permafrost in the more northerly regions, NE, BM and CM, is the main cause of differences in the average hydrologic conditions in these regions as compared with more southerly regions, SM and WF, as summarized in Table VI. While it is not clear how long permafrost thaw will continue to augment discharge in these systems, it is likely that future patterns in the post-thaw phase will perhaps mimic hydrology in the more southerly regions.

While previous studies have documented hydrologic and water balance impacts on lakes related to permafrost thaw (Prowse *et al*., 2006), few large basin studies have found distinctive trends (Peterson *et al*., 2002; Berezovskaya *et al*., 2004) that have been attributed to permafrost thaw occurring over relatively small areas such that it does not fundamentally alter the water storage or water balance of the whole basin (see Karlsson *et al*., 2012). This study benefits from finer spatial resolution made possible because of the use of an isotopic method and longer-term weighting of the records over the residence time of water in the lakes. We do not observe a decrease in inter-annual variability in thaw lakes noted as a permafrost degradation signal in some basins (Ye *et al*., 2009). In contrast, we find inter-annual variability to be relatively similar in all lakes. Other indicators of permafrost degradation such as higher peak flows and lower base flows (Karlsson *et al*., 2012) were not observable from the current dataset.

CONCLUSIONS AND IMPLICATIONS

Hydrology in the study region is driven by a combination of factors including land cover, watershed morphometry and climatic drivers. While similar patterns have been noted in some previous studies of wetland-dominated catchments (Prepas *et al*., 2001; Gibson *et al*., 2002), long-term estimates of hydrological parameters produced in this study improve our understanding of the hydrological regime of various lake subregions, many of which are under imminent pressure from planned oil sands development. In fact, Kearl L. (NE11) has already been developed as part of a recent oil sands expansion. Site-specific water yield estimates have also been incorporated into critical loads assessments for the region to improve upon less reliable estimates obtained by interpolating from a sparse hydrometric gauging network (see Bennett *et al*., 2008; Gibson *et al*., 2010a). Of particular importance, we also document and preliminarily quantify the specific influence of permafrost thaw on many lakes that was previously unknown. This aspect of our study only became apparent as a consequence of efforts directed towards better mapping of wetland-dominated land cover for watersheds across the region.

Permafrost thaw in bogs, occurring in the region since the Little Ice Age and in particular over the last 100 years (Vitt *et al*., 1994), appears to have a substantial influence on the hydrology of lakes in northeastern Alberta. While permafrost meltwater water is not directly labelled by a distinct isotopic composition but is rather similar to mean annual precipitation, this similarity allows for more reliable application of the isotope mass balance model to predict the amount effect of permafrost thaw on runoff. We estimate that up to several hundred millimetres per year of sustained runoff is being generated from permafrost thaw of peat plateaus in higher elevation ranges of the BM, in CM and in NE. Clearly, understanding of the permafrost degradation process in the region would benefit from additional field work to directly characterize the processes operating in the thaw lakes and to better understand the likely impacts of eventual decline in meltwater sources. Such impacts may include lower water levels, reduced runoff and/or lake acidification. These are major objectives of ongoing and proposed research in the region. The method could also be suitably applied more widely across the northern cold-regions to characterize runoff and to study processes such as permafrost degradation.

ACKNOWLEDGEMENTS

We thank Rose Bloise (Southern Illinois University) for her wetland mapping results for the RAMP lakes and Scott Jascechko, Dioni Cendon and Kevin Tattrie for assisting with groundwater and permafrost sampling programs. We thank Preston McEachern, Rod Hazewinkel and other staff from Alberta Environment and Sustainable Resource Development for providing lake water samples. Paul Eby (Alberta Innovates Technology Futures) and staff of the Environmental Isotope Laboratory, University of Waterloo provided analytical support. Funding for the hydrological assessment was provided through grants to J. J. G from Alberta Innovates Technology Futures, the Cumulative Environmental Management Association and Natural Sciences and Engineering Research Council of Canada (Discovery and Collaborative Research and Development CRDPJ 357130-07). Funding for the watershed mapping component of this paper was provided through a grant to D. H. V from the Cumulative Environmental Management Association, for which we are grateful.

REFERENCES

Beilman DW, Vitt DH, Halsey LA. 2000. Localized permafrost peatlands in western Canada: definition, distributions, and degradation. *Arctic, Antarctic, and Alpine Research* **33**: 70–77.

Bennett KE. 2006. Regional hydrologic controls on acid-sensitivity of lakes in boreal Canada: an isotopic perspective. M.Sc. Thesis, University of Victoria.

Bennett KE, Gibson JJ, McEachern PM. 2008. Water-yield estimates for critical loadings assessment: comparisons of gauging methods versus an isotopic approach. *Canadian Journal of Fisheries and Aquatic Sciences* **65**: 83–99.

Berezovskaya S, Yang D, Kane DL. 2004. Compatibility analysis of precipitation and runoff trends over the large Siberian watersheds. *Geophyscial Research Letters* **31**, L21502. DOI: 10.1029/2004GL021277, 2004

Birks SJ, Gibson JJ. 2009. Isotope hydrology research in Canada, 2003–2007. *Canadian Water Resources Journal* **34**(2): 163–176.

Bowen GJ, Wilkinson B. 2002. Spatial distribution of $\delta^{18}O$ in meteoric precipitation. *Geology* **30**: 315–318.

Brock BE, Yi Y, Clogg-Wright KP, Edwards TWD, Wolfe BB. 2009. Multi-year landscape-scale assessment of lakewater balances in the Slave River Delta, NWT, using water isotope tracers. *Journal of Hydrology* **379**: 81–91.

Canada, Energy Mines and Resources. 1978. Annual Runoff, Plate 24 In: Hydrological Atlas of Canada, Minister of Supply and Services Canada, Ottawa.

Coplen TB. 1996. New guidelines for reporting stable hydrogen, carbon, and oxygen isotope-ratio data. *Geochimica et Cosmochimica Acta* **60**: 3359–3360.

Craig H. 1961. Isotopic variations in meteoric waters. *Science* **133**: 1702–1703.

Craig H, Gordon LI. 1965. Deuterium and oxygen-18 in the ocean and marine atmosphere. In *Stable Isotopes in Oceanographic Studies and Paleotemperatures*, Tongiorgi E (ed). Spoleto: Italy; 9–130.

Gibson JJ, Birks SJ, Jeffries DS, Kumar S, Scott KA, Aherne J, Shaw P. 2010a. Site-specific estimates of water yield applied in regional acid sensitivity surveys across western Canada. *Journal of Limnology* **69**(Suppl. 1): 67–76.

Gibson JJ, Birks SJ, Kumar S, McEachern P, Hazewinkel R. 2010b. Interannual variations in water yield to lakes in northeastern Alberta: implications for estimating critical loads of acidity. *Journal of Limnology* **69**(Suppl. 1): 126–134.

Gibson JJ, Edwards TWD, Birks SJ, St. Amour NA, Buhay W, McEachern P, Wolfe BB, Peters DL. 2005. Progress in isotope tracer hydrology in Canada. *Hydrological Processes* **19**: 303–327.

Gibson JJ, Prepas EE, McEachern P. 2002. Quantitative comparison of lake throughflow, residency, and catchment runoff using stable isotopes: modelling and results from a survey of boreal lakes. *Journal of Hydrology* **262**: 128–144.

Gibson JJ, Reid R. 2014. Water balance along a chain of tundra lakes: a 20-year isotopic perspective. *Journal of Hydrology* **519**: 2148–2164.

Gonfiantini R. 1986. Environmental isotopes in lake studies. In *Handbook of Environmental Isotope Geochemistry*, Vol. **3**, Fritz P, Fontes JCh (eds). Elsevier: New York; 113–168.

Halsey LA, Vitt DH, Beilman D, Crow S, Mehelcic S, Wells R. 2003. *Alberta Wetlands Inventory Standards Version 2.0*. Alberta Sustainable Development, Resource Data Branch, Strategic Corporate Services Division, Alberta Sustainable Resource Development: Edmonton; 1–54.

Horita J, Rozanski K, Cohen S. 2008. Isotope effects in the evaporation of water: a status report of the Craig–Gordon model. *Isotopes in Environment and Health Studies* **44**: 23–49.

Jeffries DS, Semkin RG, Gibson JJ, Wong I. 2010. Recently surveyed lakes in northern Manitoba and Saskatchewan, Canada: characteristics and critical loads of acidity. *Journal of Limnology* **69**(Suppl. 1): 45–55.

Karlsson JM, Lyon SW, Destouni G. 2012. Thermokarst lake, hydrological flow and water balance indicators of permafrost change in Western Siberia. *Journal of Hydrology* **464–465**: 459–466.

Kienzle SW, Mueller M. 2013. Mapping Alberta's surface water resources for the period 1971–2000. *The Canadian Geographer* **57**: 506–518.

Mesinger F, DiMego G, Kalnay E, Mitchell K, Shafran PC, Ebisuzaki W, Jovic D, Woollen J, Rogers E, Berbery EH, Ek MB, Fan Y, Grumbine R, Higgins W, Li H, Lin Y, Manikin G, Parrish D, Shi W. 2006. North American Regional Reanalysis: a long-term, consistent, high-resolution climate dataset for the North American domain, as a major improvement upon the earlier global reanalysis datasets in both resolution and accuracy. *Bulletin of the American Meteorological Society* **87**: 343–360.

Peterson BJR, Holmes RM, McClelland JW, Vorosmarty CJ, Lammers RB, Shiklomanov AI, Shiklowmanov IA, Rahmstorf S. 2002. Increasing discharge to the Arctic Ocean. *Science* **298**: 2171–2173.

Prepas EE, Planas D, Gibson JJ, Vitt DH, Prowse TD, Dinsmore WP, Halsey LA, McEachern PM, Paquet S, Scrimgeour GJ, Tonn WM, Paszkowski CA, Wolfstein K. 2001. Landscape variables influencing nutrients and phytoplankton communities in boreal plain lakes of northern Alberta: a comparison of wetland- and upland-dominated catchments. *Canadian Journal of Fisheries and Aquatic Sciences* **58**: 1286–1299.

Prowse TD, Wrona FJ, Reist JD, Gibson JJ, Hobbie JE, Levesque LMJ, Warwick FV. 2006. Climate change effects on hydroecology of Arctic freshwater ecosystems. *Ambio* **35**: 347–358.

Quinton WL, Hayashi M. 2008. Recent advances toward physically-based runoff modeling of the wetland-dominated central Mackenzie River Basin, Chapter 14. In *Cold Region Atmospheric and Hydrologic Studies, The Mackenzie GEWEX Experience*, Woo M-K (ed), Hydrological Processes Vol. **2**; Springer-Verlag: Berlin; 257–279.

Schmidt A, Gibson JJ, Santos IR, Shubert M, Tattrie K, Weiss H. 2010. The contribution of groundwater discharge to the overall water budget of lakes in Alberta/Canada estimated from a radon mass balance. *Hydrology and Earth Systems Sciences* **14**: 79–89.

Scott KA, Wissel B, Gibson JJ, Birks SJ. 2010. Limnological characteristics and acid sensitivity of boreal headwater lakes in northwest Saskatchewan, Canada. *Journal of Limnology* **69**(Suppl. 1): 33–44.

Spangenberg JE. 2012. Caution on the storage of waters and aqueous solutions in plastic containers for hydrogen and oxygen stable isotope analysis. *Rapid Communications in Mass Spectrometry* **26**: 2627–2636.

Tattrie K. 2011. Groundwater surface water interactions in a wetland rich, low relief boreal environment. M.Sc. Thesis, University of Victoria, p.21.

Turner KW, Wolfe BB, Edwards TWD, Latz TC, Hall RI, Laroque G. 2014. Controls on water balance of shallow thermokarst lakes and their relations with catchment characteristics: a multi-year landscape-scale assessment based on water isotope tracers and remote sensing in Old Crow Flats, Yukon (Canada). *Global Change Biology* **20**: 1585–1603. DOI:10.111/gcb.12465.

Vitt DH, Halsey LA, Zoltai SC. 1994. The bog landforms of continental western Canada in relation to climate and permafrost patterns. *Arctic and Alpine Research* **26**: 1–13.

Vitt DH, Halsey LA, Zoltai SC. 1999. The changing landscape of Canada's western boreal forest: the current dynamics of permafrost. *Canadian Journal of Forest Research* **30**: 283–287.

Wolfe BB, Light EM, Macrae ML, Hall RI, Eichel K, Jasechko S, White J, Fishback L, Edwards TWD. 2011. Divergent hydrological responses to 20^{th} century climate change in shallow tundra ponds, western Hudson Bay Lowlands. *Geophysical Research Letters* **38** L23402.

Ye B, Yang D, Zhang Z, Kane DL. 2009. Variation of hydrological regime with permafrost coverage over Lena basin in Siberia. *Journal of Geophyscal Research* **107**, D234694.

Yi Y, Brock BE, Falcone MD, Wolfe BB, Edwards TWD. 2008. A coupled isotope tracer method to characterize input water to lakes. *Journal of Hydrology* **350**: 1–13.

